CORRESPONDENCE

Erlotinib in Lung Cancer

TO THE EDITOR: Shepherd and colleagues (July 14 issue)[1] report that erlotinib prolongs survival in non–small-cell lung cancer, as compared with placebo, after the failure of first-line or second-line chemotherapy. One disturbing aspect of this trial is that some patients underwent only one prior chemotherapy regimen before randomization. These same authors previously reported that docetaxel is superior to best supportive care after first-line chemotherapy.[2] Subsequent studies have confirmed the efficacy of docetaxel and shown that pemetrexed achieves similar results.[3] Did Shepherd and colleagues think that random assignment to placebo after the failure of first-line chemotherapy was ethically justifiable? The only patients for whom one could justify the assignment to placebo were those with a performance status of 3, who made up only 8.6 percent of all patients. Contrary to the authors' claim that inclusion of a placebo group was ethical, we believe that some patients were denied a therapeutic option known to be effective. Furthermore, the overall survival in the erlotinib group was inferior to that in published results with docetaxel and pemetrexed, suggesting that erlotinib should be used as third-line chemotherapy.

Chadi Nabhan, M.D.
Jacob D. Bitran, M.D.

Lutheran General Cancer Institute
Park Ridge, IL 60068
cnabhan@oncmed.net

Dr. Nabhan reports being an investigator in a study that is sponsored by Sanofi-Aventis.

1. Shepherd FA, Rodrigues Pereira JR, Ciuleanu T, et al. Erlotinib in previously treated non–small-cell lung cancer. N Engl J Med 2005; 353:123-32.
2. Shepherd FA, Dancey J, Ramlau R, et al. Prospective randomized trial of docetaxel versus best supportive care in patients with non-small-cell lung cancer previously treated with platinum-based chemotherapy. J Clin Oncol 2000;18:2095-103.
3. Hanna N, Shepherd FA, Fossella FV, et al. Randomized phase III trial of pemetrexed versus docetaxel in patients with non-small-cell lung cancer previously treated with chemotherapy. J Clin Oncol 2004; 22:1589-97.

TO THE EDITOR: Shepherd et al. and Tsao et al.[1] (July 14 issue) report an important study (BR.21) showing a survival benefit of erlotinib, but the results of the molecular analysis confused us. Recent East Asian studies[2-4] have strongly suggested that the mutational status of the epidermal growth factor receptor (EGFR) is the major determinant of tumor response and survival in patients with non–small-cell lung cancer who are treated with gefitinib, another EGFR tyrosine kinase inhibitor. Response rates among patients with an EGFR mutation were consistently higher than 80 percent in those studies. However, in the BR.21 study, the response rate among such patients was only 16 percent, and mutational status had no significant effect on survival, although the EGFR copy number correlated with responsiveness and survival. In our study,[2] the EGFR copy number was associated with gefitinib sensitivity, but we consider it to be a surrogate marker for EGFR mutations, rather than a true determinant.

These discrepancies may be due to differences in the ethnic background of the populations, the drugs, the study design, and, most important, the accuracy of the molecular analyses. To avoid fruitless controversy, standard methods for analyzing EGFR mutations and copy number should be established.

Toshimi Takano, M.D.
Yuichiro Ohe, M.D.
National Cancer Center Hospital
Tokyo 104-0045, Japan
yohe@ncc.go.jp

1. Tsao M-S, Sakurada A, Cutz JC, et al. Erlotinib in lung cancer — molecular and clinical predictors of outcome. N Engl J Med 2005; 353:133-44.
2. Takano T, Ohe Y, Sakamoto H, et al. Epidermal growth factor receptor gene mutations and increased copy numbers predict gefitinib sensitivity in patients with recurrent non-small-cell lung cancer. J Clin Oncol (in press).
3. Mitsudomi T, Kosaka T, Endoh H, et al. Mutations of the epidermal growth factor receptor gene predict prolonged survival after gefitinib treatment in patients with non-small-cell lung cancer with postoperative recurrence. J Clin Oncol 2005;23:2513-20.
4. Han S-W, Kim T-Y, Hwang PG, et al. Predictive and prognostic impact of epidermal growth factor receptor mutation in non-small-cell lung cancer patients treated with gefitinib. J Clin Oncol 2005;23: 2493-501.

TO THE EDITOR: Tsao and colleagues suggest that EGFR mutations were not valuable in predicting a benefit of erlotinib in the BR.21 trial. We believe that the mutation data in their report are inconclusive, for several reasons.

First, in Europe and North America,[1,2] the frequency of mutations is approximately 10 percent; Tsao et al. report mutations in more than 20 percent of the tumors. Second, only 47 percent of the mutations reported were drug-sensitive exon 19 deletions and L858R substitutions; these make up approximately 90 percent of the EGFR mutations in aggregate in the published data.[3] Third, the remaining cases showed "novel variant" mutations whose somatic nature was not established and that were not adequately confirmed. Fourth, these novel mutations were predominantly nucleotide transitions (92 percent), suggesting they were artifacts generated in the polymerase chain reaction (PCR).[4]

Finally, of the 427 patients treated with erlotinib, only 19 who had EGFR mutations could be evaluated. Among these 19 patients, only 8 had tumors with the well-established, drug-sensitive EGFR mutations. At our institution, 33 patients who had tumors containing one of these two common mutations have received erlotinib or gefitinib, and of these, 32 patients (97 percent) have had a response according to the Response Evaluation Criteria in Solid Tumors; the aggregate published response rate for both drugs and mutations is nearly 80 percent.

William Pao, M.D., Ph.D.
Marc Ladanyi, M.D.
Vincent A. Miller, M.D.
Memorial Sloan-Kettering Cancer Center
New York, NY 10021
paow@mskcc.org
for the Lung Cancer Oncogenome Group

1. Eberhard DA, Johnson BE, Amler LC, et al. Mutations in the epidermal growth factor receptor and in KRAS are predictive and prognostic indicators in patients with non-small-cell lung cancer treated with chemotherapy alone and in combination with erlotinib. J Clin Oncol 2005;23:5900-9.
2. Pao W, Miller V, Zakowski M, et al. EGF receptor gene mutations are common in lung cancers from "never smokers" and are associated with sensitivity of tumors to gefitinib and erlotinib. Proc Natl Acad Sci U S A 2004;101:13306-11.
3. Pao W, Miller VA. Epidermal growth factor receptor mutations, small molecule kinase inhibitors, and non-small-cell lung cancer: current knowledge and future directions. J Clin Oncol 2005;23: 2556-68.
4. Wong C, DiCioccio RA, Allen HJ, Werness BA, Piver MS. Mutations in BRCA1 from fixed, paraffin-embedded tissue can be artifacts of preservation. Cancer Genet Cytogenet 1998;107:21-7.

DRS. SHEPHERD AND SEYMOUR REPLY: Patients entering the BR.21 trial after first-line chemotherapy were considered by their doctors not to be suitable candidates for second-line chemotherapy. Physicians had to attest to this, and reasons were recorded and monitored. Thus, these patients could not be compared with patients who participated in the trials cited by Drs. Nabhan and Bitran. We think, therefore, as did ethics review boards and regulatory authorities, that the inclusion of a placebo-control group was ethical, since further chemotherapy was not an option and alternative systemic treatments were unavailable.

It is inappropriate to compare the results of the BR.21, TAX 317,[1] and JMEI[2] trials, since their patient populations differed considerably. One third of the patients in the BR.21 study had a performance status of between 2 and 3 or 3, as compared with 25 percent of those in the TAX 317 trial and 12 percent of those in the JMEI study. Survival shortens with each successive chemotherapy regimen. In JMEI and TAX 317, 100 percent and 75 percent of patients, respectively, had undergone only one regimen, as compared with 50 percent of the patients in the BR.21 trial. These imbalances in prognostic factors alone could result in shorter survival, independent of treatment.

With regard to patients who were not eligible

for second-line chemotherapy, we think that EGFR inhibitor therapy is ethical on the basis of the BR.21 trial. Whether it should be considered electively for patients who are otherwise suitable candidates for chemotherapy awaits the results of an ongoing study comparing docetaxel with gefitinib.

Frances A. Shepherd, M.D.

Princess Margaret Hospital
Toronto, ON M5G 2MP, Canada

Lesley Seymour, M.D.

National Cancer Institute of Canada Clinical Trials Group
Kingston, ON K7L 3N6, Canada

1. Shepherd FA, Dancey J, Ramlau R, et al. Prospective randomized trial of docetaxel versus best supportive care in patients with non-small-cell lung cancer previously treated with platinum-based chemotherapy. J Clin Oncol 2000;18:2095-103.
2. Hanna N, Shepherd FA, Fossella FV, et al. Randomized phase III trial of pemetrexed versus docetaxel in patients with non-small-cell lung cancer previously treated with chemotherapy. J Clin Oncol 2004;22:1589-97.

DR. TSAO AND COLLEAGUES REPLY: Of 177 tumor samples analyzed in the BR.21 trial, 21 samples (from 20 patients) were exon 19 deletions or L858R substitutions. This rate per patient of 11 percent for classic mutations is similar to that in other reports involving non-Asian patients.[1,2] The response rate among patients who could be evaluated who had classic mutations was 25 percent (two of eight). Although the rate is lower than that among Asian patients, it probably falls within the confidence interval of other series involving non-Asian patients who did not have adenocarcinoma.

The patients in the BR.21 trial who had classic mutations did not derive a greater survival benefit from erlotinib (hazard ratio for death, 0.67) than those with novel mutations (hazard ratio, 0.65) or those with wild-type EGFR (hazard ratio, 0.73). In the Tarceva Responses in Conjunction with Taxol and Carboplatin (TRIBUTE) trial,[3] 29 of 274 (11 percent) of the samples contained mutations (86 percent were classic mutations). Patients who had mutations had longer progression-free survival ($P<0.001$) and overall survival ($P<0.001$) than those who did not have mutations, regardless of the type of treatment (chemotherapy with or without erlotinib); the benefit of erlotinib was statistically nonsignificant. Among patients in the placebo group, those with classic mutations had a longer median survival than those with wild-type or novel EGFR variants (9.1, 3.5, and 3.5 months, respectively). This suggests that classic EGFR mutations have a prognostic influence that is independent of treatment and that the superior survival reported for mutation-positive patients in uncontrolled studies may not have been due to heightened sensitivity to the EGFR inhibitor.

Dr. Pao and colleagues suggested that novel variants are PCR artifacts caused by formalin fixation. The probability of the appearance of PCR artifacts correlates inversely with the number of cells used for the PCR.[1] However, we found novel mutations more frequently in large biopsy or resection specimens (61 percent) than in small biopsy specimens (41 percent). Chou et al.[4] also identified several new mutations (V689M, N700D, S720P, V765A, T783A, and G863D) in formalin-fixed tumors from patients who had a response, and the one patient in our series who had a complete response had a transition mutation (V742A[T→C]).

The role of mutations in patients with lung cancer receiving EGFR inhibitors is still evolving. We elected to publish all our mutation results and encourage others to do so as well. Only in this way will sufficient numbers accrue for all mutations to permit clinical correlation. We agree with Takano and Ohe that standard methods for EGFR-mutation analysis and copy number should be established. It is premature to say that EGFR-inhibitor therapy should not be prescribed for patients who do not have EGFR mutations.

Ming-Sound Tsao, M.D.
Suzanne Kamel-Reid, Ph.D.
Frances A. Shepherd, M.D.

Princess Margaret Hospital
Toronto, ON M5G 2M9, Canada

1. Cappuzzo F, Hirsch FR, Rossi E, et al. Epidermal growth factor receptor gene and protein and gefitinib sensitivity in non-small-cell lung cancer. J Natl Cancer Inst 2005;97:643-55.
2. Williams C, Pontén F, Moberg C, et al. A high frequency of sequence alterations is due to formalin fixation of archival specimens. Am J Pathol 1999;155:1467-71.
3. Eberhard DA, Johnson BE, Amler LC, et al. Mutations in the epidermal growth factor receptor and in KRAS are predictive and prognostic indicators in patients with non-small-cell lung cancer treated with chemotherapy alone or in combination with erlotinib. J Clin Oncol 2005;23:5900-9.
4. Chou T-Y, Chiu C-H, Li L-H, et al. Mutation in the tyrosine kinase domain of epidermal growth factor receptor is a predictive and prognostic factor for gefitinib treatment in patients with non-small cell lung cancer. Clin Cancer Res 2005;11:3750-7.

Phase II trial of postoperative adjuvant cisplatin and etoposide in patients with completely resected stage I-IIIa small cell lung cancer: The Japan Clinical Oncology Lung Cancer Study Group Trial (JCOG9101)

Ryosuke Tsuchiya, MD,[a] Kenji Suzuki, MD,[a] Yukito Ichinose, MD,[b] Yoh Watanabe, MD,[c] Tsutomu Yasumitsu, MD,[d] Naoki Ishizuka, PhD,[e] and Harubumi Kato, MD[f]

Objective: Indications for surgical intervention for very limited small cell lung cancer have not yet been determined. The objective of this study is to determine whether resection followed by cisplatin and etoposide is feasible.

Methods: From September 1991 through December 1996, 62 patients with completely resected small cell lung cancer who were less than 76 years of age from 17 centers were entered in the trial. Of 62 patients, 61 were eligible, with a median follow-up of 65 months. Chemotherapy consisted of 4 cycles of cisplatin (100 mg/m^2, day 1) and etoposide (100 mg/m^2, days 1-3). There were 49 (80%) male patients, 44 with clinical stage I disease, 10 with stage II disease, and 6 with stage IIIa disease.

Results: Forty-two (69%) patients received 4 cycles of cisplatin and etoposide. No treatment-associated mortality was noted. Median survival time was not reached in patients with pathologic stage I disease, was 449 days in patients with stage II disease, and was 712 days in patients with stage IIIa disease. Three-year survival was 61% overall, 68% in patients with clinical stage I disease, 56% in patients with stage II disease, and 13% in patients with stage IIIa disease ($P = .02$). Recurrence was noted in 26 (43%) patients overall. Local failure was noted in 6 (10%) patients. Locoregional recurrence tends to be found more frequently in patients with stage IIIA disease. Distant failure was found in 21 (34%) patients overall. Brain metastasis was found in 15% of the patients.

Conclusion: Major lung resection followed by postoperative cisplatin and etoposide is feasible, with a favorable survival profile. Because nodal metastasis appears to be a major prognostic factor, preoperative evaluation of nodal status remains a major concern.

From the Division of Thoracic Surgery,[a] National Cancer Center Hospital, Tokyo; the Department of Thoracic Oncology of the National Kyushu Cancer Center,[b] Kyushu; the Department of Surgery of the University of Kanazawa,[c] Kanazawa; the Department of Surgery of the Habikino Hospital,[d] Osaka; the JCOG Data Center of the National Cancer Center,[e] Tokyo; the Department of Surgery of the Tokyo Medical College,[f] Tokyo, Japan; and the Lung Cancer Surgical Study Group of Japan Clinical Oncology Group.

Supported in part by a Grant-in-Aid for Cancer Research from the Ministry of Health and Welfare.

Received for publication Sept 3, 2003; revisions received April 21, 2004; accepted for publication May 6, 2004.

Address for reprints: Ryosuke Tsuchiya, MD, Thoracic Surgery Division, National Cancer Center Hospital, 1-1, Tsukiji 5 cho-me, Chuo-ku, Tokyo 104-0045 Japan (E-mail: rtsuchiy@ncc.go.jp).

J Thorac Cardiovasc Surg 2005;129:977-83

0022-5223/$30.00

doi:10.1016/j.jtcvs.2004.05.030

The prognosis of lung cancer remains poor, and this disease is the leading cause of cancer mortality worldwide. Small cell lung cancer (SCLC) comprises approximately 20% of lung cancer cases. Without treatment, SCLC has the most aggressive clinical course of any other type of lung cancer, resulting in a very short median survival time of approximately 2 to 4 months. Although surgical resection is generally indicated for early stage non–small cell lung cancer, this is not always the case with SCLC. This can be explained by the fact that

dissemination to regional lymph nodes or distant organs would be found in most patients with SCLC at the time of initial presentation.[1] Therefore, localized forms of treatment, such as surgical resection or radiation therapy, rarely produce long-term survival, and systemic treatment with current chemotherapy regimens is usually incorporated into the treatment program.

Indications for surgical resection for SCLC have not yet been determined, although several authors have reported that a small minority of patients with limited-stage disease and adequate lung function might benefit from surgical resection.[1-9] According to these reports, the prognosis of resected SCLC was not so poor, especially when no pathologic nodal involvement was observed. The 5-year survival ranged from 26% to 61% in these trials if the tumor was stage I. Because SCLC tends to be disseminated and the results of surgical intervention alone for this disease have been reported to be poor,[1,10] postoperative chemotherapy has been used in most studies. However, the chemotherapy was not standardized, and various chemotherapy protocols were often used. Furthermore, most previous studies were retrospective and thus suffered from the inherent weakness of any retrospective assessment of a given treatment.

Because the combination of cisplatin and etoposide has been considered to be standard in the treatment of SCLC,[11] this combination was selected as a postoperative adjuvant regimen. We conducted a prospective study of surgical resection plus adjuvant chemotherapy for stage I through IIIA SCLC to investigate the efficacy of this treatment strategy.

Patients and Methods

Eligibility

Patients who were given postoperative diagnoses of SCLC histologically or cytologically were eligible for enrollment in the study. The patients had to have completely resected pathologic stage I, II, or IIIA disease according to the TNM classification of the International Union Against Cancer.[12] Histologic typing was determined according to the World Health Organization classification.[13] Inclusion criteria included an Eastern Cooperative Oncology Group performance score of 0 or 1, age between 20 and 75 years, no prior treatment for lung cancer, no other concurrent or previous malignancies, a leukocyte count of greater than 3500/μL, a platelet count of greater than 100,000/μL, a hemoglobin level of greater than 9.5 g/dL, a serum creatinine level of less than 1.5 mg/dL, and aspartate aminotransferase–alanine aminotransferase values of less than twice the institutional upper limit of normal. Exclusion criteria included a history of myocardial infarction within the past 3 months, hepatic cirrhosis, and/or severe cardiopulmonary dysfunction that required oxygen therapy. The following preoperative investigations were performed before entry into the study: computed tomographic (CT) scanning of the chest, upper abdomen, and brain; bronchoscopy; chest plain film; radionuclide bone scanning; complete blood cell count and serum chemistry; and physical examination. Preoperative mediastinoscopy was performed in some cases. All patients provided written informed consent before entering the study.

Treatment Schedule

Major lung resection, such as pulmonary lobectomy or pneumonectomy, was required as a surgical procedure for SCLC. Complete hilar and mediastinal lymph node dissections were recommended on the basis of the lymph node map defined by Naruke and colleagues.[14] After confirming complete resection and histologic typing of SCLC histologically, eligible patients were registered in the study.

Chemotherapy consisted of cisplatin (100 mg/m^2 on day 1) and etoposide (100 mg/m^2 on days 1-3; PE regimen). This regimen was repeated every 4 weeks and was administered in 4 courses. The dose was modified according to the blood cell count and renal function on the day of chemotherapy. Chemotherapy was administered unless the leukocyte count was less than 3000/μL or the platelet count was less than 75,000/μL. Chemotherapy was withheld until the counts recovered. If grade 4 hematologic toxicity, according to World Health Organization (WHO) criteria,[15] was seen, the dose of etoposide was reduced to 75%. Chemotherapy was permanently discontinued at any time when the serum creatinine level was 2.0 mg/dL or greater or the blood urea nitrogen level was 30 mg/dL or greater. To assess toxicity, we subjected all patients to complete blood cell counts and blood chemistry evaluations, such as for aspartate aminotransferase–alanine aminotransferase, blood urea nitrogen, and serum creatinine, as well as chest plain film and urinalyses at least once per week during treatment. Toxicity criteria were evaluated on the basis of the WHO criteria.[15]

Patients were followed up at the outpatient department every 3 months postoperatively and underwent CT scans of the chest, upper abdomen, and brain, as well as radionuclide bone scanning every 6 months, even when they were asymptomatic. No postoperative radiotherapy was applied until relapse was apparent.

Sites of relapse were determined by clinical, radiologic, or histologic criteria at initial recurrence. Local failure was defined as recurrence at the primary lung site or hilar-mediastinal lymph nodes. Distant failure was defined as recurrence in the contralateral lung, bone, brain, liver, or other extrathoracic regions.

Statistical Analysis

The trial was designed as a prospective phase II trial. The primary goal of the study was to estimate the survival. A sample size of 30 was considered to provide a power of 90% for detecting a significant improvement in the 3-year survival (from 20% to 50%) in a 1-sided test with an α value of .025 and a β value of .10. The median follow-up period for 35 surviving patients was 65 months. The length of survival was defined as the interval in months between the day of surgical resection of lung cancer and the date of death from any cause or the last follow-up. The survival curves were constructed by using the Kaplan-Meier method,[16] and curves were compared with the log-rank test.

Results

Patient Characteristics

Between September 1991 and December 1996, 62 patients were entered in this phase II trial at the 16 institutions that

TABLE 1. Patient characteristics

Total	61
Sex	
Male	49
Female	12
Age (y)	
Range	22-74
Median	64
Histologic subtype defined by WHO*	
Oat cell type	9
Intermediate type	45
Combined type	7
Clinical stage	
I	44
II	9
IIIA	8
Side of primary tumor	
Right	32
Left	29
Operative procedure	
Lobectomy	57
Pneumonectomy	4
Extent of lymph node dissection†	
Complete hilar and mediastinum	59
Only hilar	2
Pathologic stage	
I	35
II	8
IIIA	18
Performance status	
0	32
1	29

*Histologic subtyping was determined on the basis of the World Health Organization (WHO) classification. †The extent of lymph node dissection was defined by Naruke and associates.[14]

participated in the study. One patient was excluded because his final histologic category was changed from SCLC to large cell carcinoma. Thus, 61 patients were eligible for assessment of survival data, and their characteristics are shown in Table 1. The median age was 64 years (range, 22-74 years). According to histologic typing defined by the WHO, oat cell, intermediate, and combined types were found in 9, 45, and 7 patients, respectively. Forty-four patients had clinical stage I disease, 9 had stage II disease, and 8 had stage IIIA disease. Pathologically, stage I, II, and IIIA disease was found in 35, 8, and 18 patients, respectively.

Treatment Administration

As a surgical procedure, pulmonary lobectomy was performed in 57 (93%) patients, and pneumonectomy was performed in the other 4 patients. Among 4 pneumonectomies, 3 were on the left side, and 1 was on the right side. Complete hilar and mediastinal lymph node dissection was performed in 59 (97%) patients.

TABLE 2. Treatment delivery

Total no. of patients	61
No. of chemotherapy courses	
0	1 (2%)
1	5 (8%)
2	8 (13%)
3	5 (8%)
4	42 (69%)

A total of 204 courses were administered (Table 2). Forty-two (69%) patients underwent a full course of chemotherapy. The other 19 patients did not complete postoperative chemotherapy because of progressive disease in 3 patients, adverse effects in 7 patients, refusal of chemotherapy in 8 patients, and death from pneumonia in 1 patient.

Treatment-Related Toxicity

No treatment-associated deaths were found. Postoperative bronchopulmonary fistula was found in 1 (2%) patient who underwent pulmonary lobectomy after completion of the first cycle of chemotherapy. Chemotherapy-related toxicity is shown in Table 3. Grade 4 toxicity was found in 9 (15%) patients: leukopenia in 4 patients, thrombocytopenia in 2 patients, nausea in 2 patients, and cardiac failure in 1 patient. One patient died of pneumonia 2 months after the first course of chemotherapy, but this was not considered to be chemotherapy related.

Survival

Survival data are shown in Table 4. Among the 61 eligible patients, 35 were still alive after a median follow-up of 65

TABLE 3. Chemotherapy-related toxicity in 60 eligible patients treated for resected stage I to IIIA SCLC

	WHO grade				
Toxicity	1	2	3	4	4 (%)
Anemia	9	29	16	0	0
Leukocytopenia	7	17	26	4	6.5
Thrombocytopenia	11	8	14	2	3.2
Infection	2	1	0	0	0
Nausea	24	13	13	2	3.3
Diarrhea	8	2	2	0	0
Azotemia	35	0	0	0	0
Renal failure	18	0	0	0	0
Stomatitis	14	1	1	0	0
Dyspnea	5	0	0	0	0
Fever	10	7	0	0	0
Skin	4	2	0	0	0
Alopecia	13	23	11	0	0
Cardiac dysfunction	5	2	1	1	1.7
CNS	1	1	1	0	0
Peripheral neuropathy	5	1	0	0	0

WHO, World Health Organization; *CNS,* central nervous system.

TABLE 4. Survival in patients with resected SCLC who underwent postoperative chemotherapy

	Median survival time (d)	Survival 3 y	Survival 5 y
Clinical stage			
IA	Not reached	70%	66%
IB	Not reached	65%	65%
II	Not reached	56%	56%
IIIA	530	13%	13%
Pathologic stage			
IA	Not reached	78%	73%
IB	Not reached	67%	67%
II	449	38%	38%
IIIA	712	39%	39%

months. The overall estimated 3- and 5-year survivals were 61% and 57%, respectively (Figure 1). The 5-year survival was 66%, 56%, and 13% in patients with clinical stage I, II, and IIIA disease, respectively (Figure 2). Among the 44 patients with clinical stage I disease, 27 were classified as having clinical stage IA disease, and the other 17 were classified as having clinical stage IB disease. There was no significant difference in prognosis between clinical stage IA and IB disease. Similar results were obtained regarding the pathologic stage. Pathologic stage I disease showed a significantly better prognosis (Figure 3). The 5-year survivals in the 23 patients with pathologic stage IA disease and the 12 patients with stage IB disease were 73% and 67%, respectively. No significant differences in survival were observed between patients with pathologic stage IA and IB disease.

Patterns of failure. Recurrence was noted in 26 (43%) patients, and the sites of initial relapse at a median follow-up time of 65 months are shown according to the pathologic stage in Table 5. Recurrence was found in 30% of patients with stage IA disease, 25% of patients with stage IB disease, 50% of patients with stage II disease, and 67% of patients with stage IIIA disease.

Local failure was noted in 6 (10%) patients: 4 in the mediastinal lymph nodes and 2 in the bronchial stump. Locoregional recurrence tended to be found more frequently in patients with stage IIIA disease (22%) than in patients with stage I or II disease. Relapse at the bronchial stump was only seen in patients with stage IIIA disease.

Distant failure was found in 22 (36%) patients overall: 6 (26%) with stage IA disease, 2 (17%) with stage IB disease, 4 (50%) with stage II disease, and 9 (50%) with stage IIIA disease. Distant failure was most frequently noted in the brain, followed by the liver. The incidence of brain metastasis was 15% overall, 17% in patients with stage IA disease, and 11% in patients with stage IIIA disease. Bone metastasis was noted exclusively in patients with stage IIIA disease.

Discrepancy between clinical and pathologic stages. Table 6 shows the relationship between the clinical stage and the pathologic stage. Among 44 patients with clinical stage I disease, only 33 (75%) had pathologic stage I disease, and

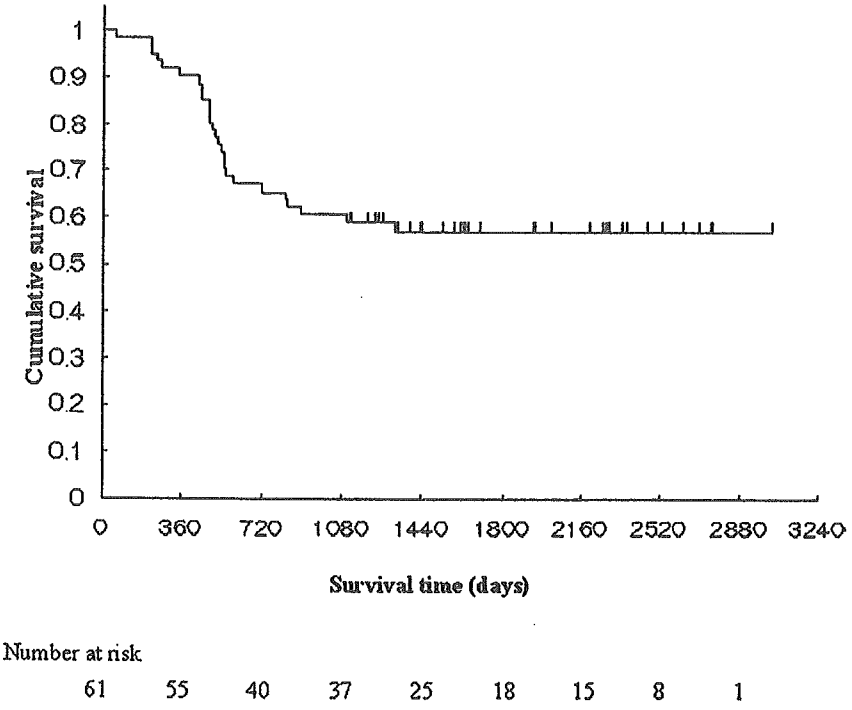

Figure 1. Survival curve for overall patients with resected SCLC.

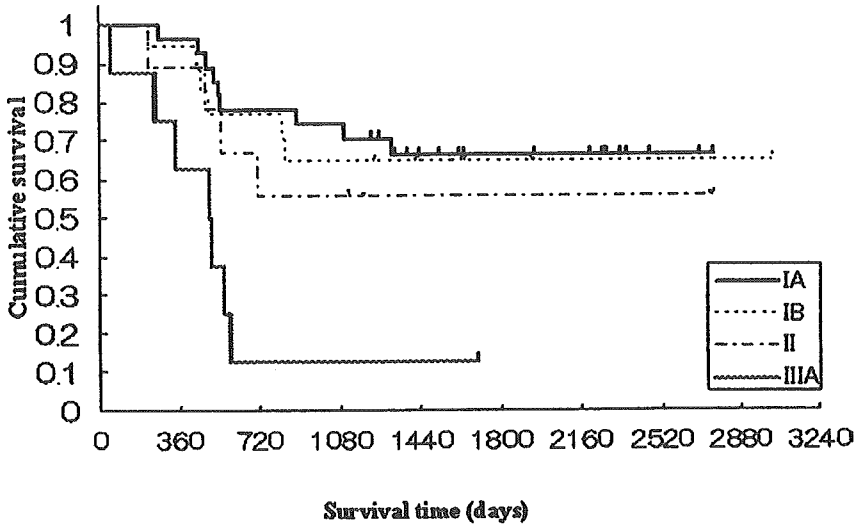

Figure 2. Survival curves for patients with resected SCLC by clinical stages.

6 had stage IIIA disease. Five patients with clinical stage IA disease had mediastinal lymph node metastasis. According to the Bowker test of symmetry, these differences were statistically significant.

Discussion

This phase II trial showed that postoperative PE for patients who underwent surgical resection of stage I to IIIA SCLC was feasible, and the outcome was acceptable. Survival was excellent in patients with stage I disease and did not appear to be inferior to that with chemoradiotherapy in patients with stage II or IIIa disease.

On the basis of the results of the British Medical Research Council, radical radiotherapy has been preferable to surgical intervention for SCLC,[17,18] and the indications for surgical resection for SCLC are still controversial. An operation would be indicated for limited SCLC because the most common relapse site after radiotherapy was locoregional, and surgical intervention might improve local control.[19] Several authors have reported that a small minority of

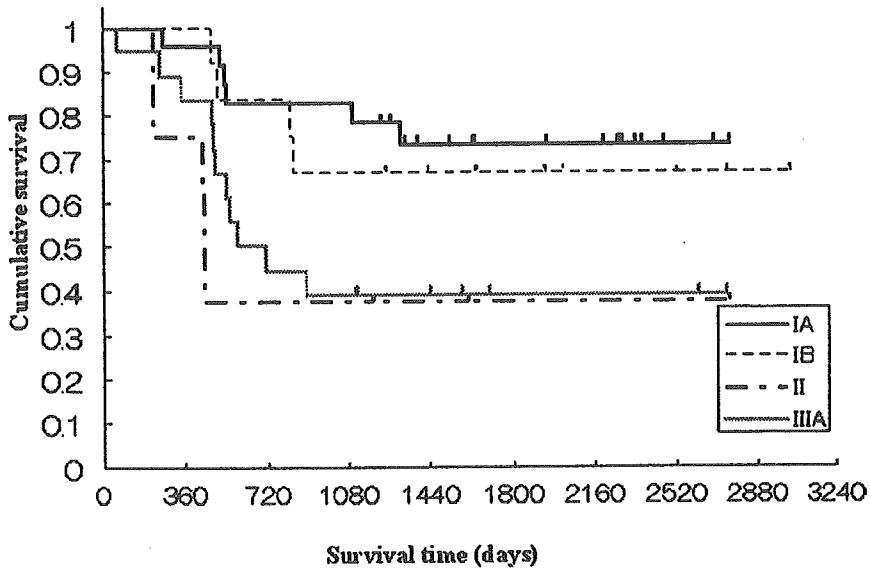

Figure 3. Survival curves for patients with resected SCLC by pathologic stage.

TABLE 5. Site of the first relapse by pathologic stages*

Variables	Overall	Stage IA	Stage IB	Stage II	Stage IIIA
No. of patients	61	23	12	8	18
No. of recurrence	26 (43%)	7 (30%)	3 (25%)	4 (50%)	12 (67%)
Recurrence					
Local					
Overall	6 (10%)	1 (4%)	1 (8%)	0 (0%)	4 (22%)
Mediastinum	4	1	1	0	2
Bronchial stump	2	0	0	0	2
Distant					
Overall	22 (36%)	6 (26%)	2 (17%)	4 (50%)	9 (50%)
Brain	9 (15%)	4 (17%)	0 (0%)	3 (38%)	2 (11%)
Bone	3	0	0	0	3
Liver	7	1	1	1	4
Lung	2	0	1	0	1
Small intestine	2	1	0	0	1

limited-stage SCLCs could be managed with an operation and postoperative chemotherapy.[1-9] According to those reports, the 5-year survivals were 28% to 36% overall and 26% to 61% in patients with stage I disease. However, most of those reports were retrospective and used various combinations of chemotherapy. Therefore, a prospective trial of adjuvant chemotherapy for patients with resected SCLC using standardized chemotherapy has been needed. Our survival data suggest that postoperative PE after major lung resection and hilar and mediastinal lymph node dissection is a feasible and promising treatment, especially for patients with stage I SCLC. The 3- and 5-year survivals for patients with stage I disease were 78% and 73%, respectively, and the median survival time was not reached. As for patients with stage II or IIIA disease, the results were not definitive, and a further prospective study is needed. This study dealt with postoperatively proved SCLC. As to the indication for surgical intervention for preoperatively diagnosed SCLC, controversies still remain. Our recommendation is as follows. When a patient has SCLC of clinical N1 or N2 status, chemoradiotherapy should be considered because a survival after an operation alone would not be good enough. Surgical intervention should be considered, however, for patients with clinical stage I disease because an operation followed by chemotherapy offers a good prognosis, as shown in this study, and because such SCLC sometimes turns out to be non-SCLC postoperatively. A phase III trial comparing chemoradiotherapy with surgical intervention followed by chemotherapy is interesting. However, the number of patients with SCLC with clinical stage I or II disease is very small, and we do not think it is possible to perform the phase III trial in this population.

TABLE 6. Relationship between clinical and pathologic stages

Clinical stage	Pathologic stage I	II	IIIA	*P* value*
I	33	5	6	.011
II	1	3	5	
IIIA	1	0	7	

*P value in Bowker's test of symmetry.

Because clinical stage and pathologic stage were significant prognostic factors in our trial, preoperative staging, intraoperative staging, or both should be a major concern for the treatment of very limited SCLC. Actually, the following preoperative investigations were performed before entry into the study in this cohort: CT scans of the chest, upper abdomen, and brain; bronchoscopy; chest plain film; radionuclide bone scans; complete blood cell count and serum chemistry; and physical examination. If the diagnosis of SCLC was made preoperatively, we recommend the same preoperative workup as done by us in this study. Furthermore, if swollen lymph nodes are detected on thoracic CT scans, we absolutely recommend mediastinoscopy for such cases. As for positron emission tomography, we have no recommendation thus far because this modality has recently begun to be evaluated, although it could be useful for staging N1 disease. Intraoperatively, hilar and mediastinal lymph node sampling or dissection was performed in 59 (97%) patients. This intraoperative staging is also important for deciding on the treatment strategy.

The site of the first relapse was another fruit of our study. This clinical trial did not use postoperative mediastinal irradiation or prophylactic cranial irradiation (PCI). We should discuss the importance of these strategies for very limited SCLC. As to locoregional recurrence, approximately 10% of the patients showed relapse in the mediastinal lymph nodes, bronchial stump, or both. Five percent of patients with stage I or II disease eventually have locore-

gional recurrence, whereas this is seen in 22% of patients with stage IIIA disease. These results suggest that patients with stage IIIA disease, at least, could benefit from postoperative mediastinal irradiation, whereas those with stage I or II disease might not need to undergo radiotherapy. Thus, postoperative chemoradiotherapy might be used in a future trial for stage IIIA disease.

Auperin and associates[20] reported that PCI improved both overall survival and disease-free survival among patients with SCLC in complete remission. Surgically resected SCLC would be considered SCLC in complete remission, and PCI would be indicated. Overall, 15% of the patients in our study showed brain metastasis. Even among patients with stage IA disease, more than 10% of the patients had brain metastasis. Therefore, PCI might be necessary for all patients with completely resected SCLC, whereas some authors have insisted that patients with pathologic stage IA SCLC can be cured without any adjuvant treatment.[19]

Noda and coworkers[21] reported that combination chemotherapy consisting of irinotecan (CPT-11) and cisplatin was superior to PE for extensive SCLC. Although concurrent radiotherapy with CPT-11 would be harmful, we would use the new regimen for very limited SCLC, especially for stage II or IIIA SCLC.

Major lung resection with complete hilar and mediastinal lymph node dissection followed by postoperative PE is a feasible treatment and results in a favorable survival profile. Survival was especially good for patients with stage I disease. Our strategy could be used as a standard treatment arm in a future trial for very limited SCLC.

We thank Ms Mieko Imai and Dr Haruhiko Fukuda, JCOG Data Center, National Cancer Center Research Institute, for their technical support in statistical analyses. We also thank Dr Hideo Kunitoh, Medical Oncology and Internal Medicine Division, National Cancer Center Hospital, for his critical discussion.

References

1. Hansen HH, Dombernowsky P, Hirsch FR. Staging procedures and prognostic features in small cell anaplastic bronchogenic carcinoma. *Semin Oncol.* 1978;5:280-7.
2. Davis S, Crino L, Tonato M, et al. A prospective analysis of chemotherapy following surgical resection of clinical stage I-II small-cell lung cancer. *Am J Clin Oncol.* 1993;16:93-5.
3. Hara N, Ichinose Y, Kuda T, et al. Long-term survivors in resected and nonresected small cell lung cancer. *Oncology.* 1991;48:441-7.
4. Karrer K, Shields TW, Denck H, et al. The importance of surgical and multimodality treatment for small cell bronchial carcinoma. *J Thorac Cardiovasc Surg.* 1989;97:168-76.
5. Macchiarini P, Hardin M, Basolo F, et al. Surgery plus adjuvant chemotherapy for T1-3N0M0 small-cell lung cancer: rationale for current approach. *Am J Clin Oncol.* 1991;14:218-24.
6. Shah SS, Thompson J, Goldstraw P. Results of operation without adjuvant therapy in the treatment of small cell lung cancer. *Ann Thorac Surg.* 1992;54:498-501.
7. Shepherd FA, Ginsberg RJ, Evans WK, et al. Reduction in local recurrence and improved survival in surgically treated patients with small cell lung cancer. *J Thorac Cardiovasc Surg.* 1983;86:498-506.
8. Shields TW, Higgins GA Jr, Matthews MJ, et al. Surgical resection in the management of small cell carcinoma of the lung. *J Thorac Cardiovasc Surg.* 1982;84:481-8.
9. Ulsperger E, Karrer K, Denck H. Multimodality treatment for small cell bronchial carcinoma. Preliminary results of a prospective, multicenter trial. The ISC-Lung Cancer Study Group. *Eur J Cardiothorac Surg.* 1991;5:306-10.
10. Martini N, Wittes RE, Hilaris BS, et al. Oat cell carcinoma of the lung. *Clin Bull.* 1975;5:144-8.
11. Fukuoka M, Furuse K, Saijo N, et al. Randomized trial of cyclophosphamide, doxorubicin, and vincristine versus cisplatin and etoposide versus alternation of these regimens in small-cell lung cancer. *J Natl Cancer Inst.* 1991;83:855-61.
12. Hermanek P, Sobin LH. UICC TNM classification of malignant tumours. 4th ed. Berlin: Springer-Verlag; 1992.
13. World Health Organization. Histological typing of lung tumors. 2nd ed. Geneva: World Health Organization; 1981.
14. Naruke T, Suemasu K, Ishikawa S. Lymph node mapping and curability at various levels of metastasis in resected lung cancer. *J Thorac Cardiovasc Surg.* 1978;76:832-9.
15. World Health Organization. WHO handbook for reporting results of cancer treatment. Geneva: World Health Organization; 1979.
16. Kaplan EL, Meier P. Nonparametric estimation for incomplete observations. *J Am Stat Assoc.* 1958;53:457-81.
17. Fox W, Scadding JG. Medical Research Council comparative trial of surgery and radiotherapy for primary treatment of small-celled or oat-celled carcinoma of bronchus. Ten-year follow-up. *Lancet.* 1973; 2:63-5.
18. Comparative trial of surgery and radiotherapy for the primary treatment of small-celled or oat-celled carcinoma of the bronchus. First report to the Medical Research Council by the working-party on the evaluation of different methods of therapy in carcinoma of the bronchus. *Lancet.* 1966;2:979-86.
19. Shepherd FA. Surgical management of small cell lung cancer. In: Pass HI, Mitchell JB, Johnson DH, et al, editors. Lung cancer: principles and practice. Philadelphia: Lippincott, Williams & Wilkins; 2000. p. 967-80.
20. Auperin A, Arriagada R, Pignon JP, et al. Prophylactic cranial irradiation for patients with small-cell lung cancer in complete remission. Prophylactic Cranial Irradiation Overview Collaborative Group. *N Engl J Med.* 1999;341:476-84.
21. Noda K, Nishiwaki Y, Kawahara M, et al. Randomized phase III study of irinotecan (CPT-11) and cisplatin versus etoposide and cisplatin in extensive-disease small-cell lung cancer: Japan Clinical Oncology Group Study (JCOG 9511) [abstract]. *Proc Am Soc Clin Oncol.* 2000;19:482a.

GTS

Diffusion-Weighted Imaging of Malignant Breast Tumors

The Usefulness of Apparent Diffusion Coefficient (ADC) Value and ADC Map for the Detection of Malignant Breast Tumors and Evaluation of Cancer Extension

Reiko Woodhams, MD, Keiji Matsunaga, MD,* Keiichi Iwabuchi, MD,† Shinichi Kan, MD,* Hirofumi Hata, RT,* Masaru Kuranami, MD,‡ Masahiko Watanabe, MD,‡ and Kazushige Hayakawa, MD**

Summary: The authors used breast diffusion-weighted imaging (DWI) to diagnose breast cancer and identify cancer extension. Isotropic DWI was performed with EPI. The apparent diffusion coefficient (ADC) value was calculated and displayed on an ADC map. The authors compared between the distribution of low ADC values and pathologic cancer extension. The mean ADC value of breast cancer was $1.12 \pm 0.24 \times 10^{-3}$ mm^2/s, which was lower than that of normal breast tissue. The ADC value for invasive ductal carcinoma was lower than that of noninvasive ductal carcinoma. The sensitivity of the ADC value for breast cancer using a threshold of less than 1.6×10^{-3} mm^2/s was 95%. Seventy-five percent of all cases showed precise distribution of low ADC value as cancer extension. The causes of underestimation were susceptibility artifact from bleeding and the limit of spatial resolution. Benign proliferative change showed a low ADC value. The authors conclude that DWI has a potential for clinical appreciation in detecting breast cancer.

Key Words: diffusion-weighted image, apparent diffusion coefficient map, malignant breast tumor, benign proliferative change, susceptibility artifact

(*J Comput Assist Tomogr* 2005;29:644–649)

Magnetic resonance imaging (MRI) is one of the diagnostic tools for breast evaluation. It has been assessed extensively as a valuable tool for breast diagnosis. MRI with enhancement provides high contrast resolution and results in high sensitivity for breast carcinoma. The utility for estimating the extension of breast carcinoma and evaluation for chemotherapy treatment is already recognized.[1–6] However, MRI has some disadvantages compared with mammography and ultrasound: it has a long scan time, the use of contrast is sometimes contraindicated because of allergy, and it is expensive. Sometimes it is difficult to differentiate a malignant lesion from a benign lesion by using a morphologic approach and enhancement pattern: benign hyperplastic change, metaplasia, and fibroadenoma sometimes show an enhancement pattern similar to that of malignancy.[7–9]

On the other hand, diffusion-weighted imaging (DWI) represents the biologic character of tissue. DWI reflects the random thermal motion of molecules (Brownian motion). Mainly the Brownian motion of protons in bulk water contributes to the signal in DWI. The apparent diffusion coefficient (ADC) is used to quantify the Brownian motion. In biologic tissue, ADC includes Brownian motion (incoherent motion) and capillary blood circulation (coherent motion). However, coherent motion is affected less with high diffusion-sensitizing factor (b-value). Decreased movement of molecules in the tissue correlates with a low ADC value.

DWI is already recognized as a first choice to diagnose brain infarction.[10] Recent improvements in hardware and imaging made with DWI have expanded its applications. Investigations have shown the possibility of using DWI on other organs to diagnose and differentiate (e.g., brain abscess, pancreas, and focal hepatic lesions).[11–14] The breast is no exception for the use of DWI adaptation. Englander et al initially studied the use of DWI for human breasts.[15] Guo et al showed the statistical difference of ADC value between malignancy and benign lesions and showed the high precision of ADC to differentiate breast tumors: sensitivity was 93% and specificity 88% with an ADC threshold of 1.30×10^{-3} mm^2/s.[16]

We analyzed the ADC value of normal mammary glands and malignant breast lesions to determine the threshold of the ADC value to distinguish between malignant lesions and normal lesions and examine the DWI sensitivity for the malignant lesions. We also compared the distribution of low ADC value on an ADC map with cancer extension of the pathologic specimen and evaluated the ability of the ADC map to analyze tumor extension. We also evaluated the pathologic phenomenon compared with an altered ADC value to research the factors affecting the ADC value.

Received for publication January 22, 2005; accepted May 18, 2005.
From the *Department of Radiology, Kitasato University School of Medicine, Kanagawa, Japan; †Department of Pathology, Kitasato University School of Medicine, Kanagawa, Japan; and ‡Department of Surgery, Kitasato University School of Medicine, Kanagawa, Japan.
Reprints: Reiko Woodhams, Kitasato University School of Medicine, 1-15-1, Kitasato, Sagamihara, Kanagawa, 228-8555, Japan (e-mail: reiko99@db3.so-net.ne.jp).

METHODS

Subjects

Seventy-six patients with breast carcinoma underwent MRI, including DWI scans. All patients were female; their age ranged from 30 to 80 years (mean 53). Tissue samples were available from each patient: 31 patients underwent Auchincloss surgery and 45 had breast-conserving surgery.

Histopathologic Data

All tissues were fixed in 10% formalin and embedded in paraffin. Four-micron-thick paraffin sections were cut every 3 to 10 mm from the excised tissues. The excised materials were sliced vertically to the lines from the tumors to the nipple side. The specimens were stained with hematoxylin and eosin. The average number of the slides per case was 13 (range 5–32). All of the specimens underwent microscopic examination. There were 66 invasive ductal carcinomas (IDCs) and 10 noninvasive ductal carcinomas (NIDCs) (Table 1). The mean size of the malignant lesions was 22 mm in diameter (range 7–70 mm).

MRI Protocol

MRI was performed on a GE Signa CV/i 1.5T Version 9.1 by using a breast coil (surface coil). Prior to DWI, FRFSE using CHESS for fat saturation in the sagittal plain was performed. After DWI in the axial plane, 3D FSPGR using Spec IR for fat saturation in the sagittal plane before and after administration of gadopentetate dimeglumine (0.2 mmol/kg) was obtained. Subtraction images were produced with 3D FSPGR for identification of enhancement. 2D FSPGR with CHESS in the axial plane was obtained after enhancement. Imaging parameters were as follows: 2D FRFSE (TR = 3,000, eff TE = 85, 256 × 192, 3 NEX), DWI [spin-echo single-shot echo planar image (EPI), motion probing gradient (MPG) were applied along the x, y, and z axes (isotopic DWI) before and after the 180-degree pulses to obtain the images used for synthesizing isotropic images, b-value 0 and 750 s/mm^2, TR/TE: 5,000/61.8, image matrix: 128 × 128, field of view: 320 mm × 240 mm, slice thickness: 6 mm, spacing: 1 mm, 5 NEX, acquisition time: 60 s], 3D FSPGR (TR = 5.7, TE = 1.2, flip angle 20 degrees, image matrix: 256 × 160, 2 NEX), 2D FSPGR (TR = 200, TE minimum, flip angle 90 degrees, image matrix: 512 × 192, 3 NEX).

TABLE 1. ADCs According to Histopathology

	n	Mean ADC Value ($\times 10^{-3}$ mm^2/sec)
DCIS	9	1.31 ± 0.57
Solid tubular Ca	23	1.13 ± 0.55
Lobular Ca	8	1.07 ± 0.56
Scirrhous Ca	17	1.07 ± 0.54
Papillotubular Ca	15	1.05 ± 0.52
Intracystic papillary Ca	1	2.5
Medullary Ca	1	1.2
SCC	1	1.1
Adenoid cystic Ca	1	1.0
Total	76	

ADC, apparent diffusion coefficient; SCC, squamous cell carcinoma.

Analysis of ADC Values

ADC values were calculated according to the formula ADC = $-(1/b)\ln(S/So)$, where So and S were the signal intensities in the region of interest (ROI), obtained with two different gradient factors (b value of 0 and 750 s/mm^2). ADC distribution was demonstrated on an ADC color map using Advantage Workstation Version 4.0 (GE). ROIs were placed in the area of malignant lesions and normal mammary gland lesions on ADC map by referring to subtraction images originating from 3D FSPGR and 2D FSPGR in the axial plane after enhancement. The sizes of the ROIs were 5 to 10 mm in diameter, depending on the size of the tumors. The ROIs of malignant lesions had to be smaller than the mass size, not including normal tissue. Two diagnostic radiologists chose the areas that showed the strongest enhancement visually, and ADC values were averaged. The size of the ROI in normal tissue was 10 mm in diameter. Each ROI was placed twice by one diagnostic radiologist, and ADC values were averaged. In addition, the ADC values between NIDC and IDC were compared. Predominant NIDC was included in the NIDC category. The threshold of the ADC value for a malignant lesion was determined as a low ADC value by the results from above.

Comparison Between ADC Map and Specimens

A radiologist retrospectively identified the area of interest on the ADC map. This was pathologically examined, and a radiologist and a pathologist investigated the relationship between the ADC map and the pathologic figures. To determine the orientation of the tumors and the breast areas on the specimens, we referred to the relationship between nipple marking and main tumor position on the excised material from surgery.

The area of low ADC values were depicted on the ADC map with a certain color and compared with tumor distribution on the specimen. The areas that were not surgically excised and not pathologically evaluated were not included in this investigation. We categorized the correlation between the ADC map and tumor extension in four groups (Table 2). In group 1, the area of low ADC value was almost the same as tumor spread. In group 2, the overdiagnosed group, the area of low ADC value was wider and more than twice the area of tumor spread. In group 3, the underdiagnosed group, the area of low ADC value was smaller and less than half of the area of tumor spread. Group 4 was the false-negative group.

Statistics

The Wilcoxon signed rank sum test was used for analyzing differences of mean ADC values for significance

TABLE 2. Classification of Groups

Group No.	Group Description	n	
1	Precise group	57	75%
2	Overdiagnosed group	15	20%
3	Underestimated group	3	4%
4	False-negative group	1	1%
	Total	76	

between breast cancer and normal breast tissue and between IDC and NIDC or predominant NIDC. The honestly significant difference (HSD) of Tukey-Kramer was used to compare the mean ADC value between solid tubular carcinoma, lobular carcinoma, scirrhous carcinoma, and papillotubular carcinoma.

RESULTS

Measurement of ADC Values

The mean ADC value of normal breast tissue was $2.05 \pm 0.27 \times 10^{-3}$ mm^2/s; that of malignant lesions was $1.12 \pm 0.24 \times 10^{-3}$ mm^2/s (Fig. 1). The difference between them was significant ($P = 0.001$). According to this result, the threshold of low ADC values for a malignant lesion was determined to be less than 1.6×10^{-3} mm^2/s. The mean ADC value for IDC was $1.09 \pm 0.23 \times 10^{-3}$ mm^2/s; that for NIDC was $1.42 \pm 0.42 \times 10^{-3}$ mm^2/s. The difference between them was significant ($P = 0.0004$) (Fig. 2). The mean ADC value for each pathologic type is shown in Table 1. Among the four major types of IDC, there was no significant difference in the ADC value.

Comparison Between ADC Map and Tumor Spread

Fifty-seven cases (75% of all cases) were in group 1. The area of low ADC value corresponded with the tumor distributions. Fourteen cases (16%) were in group 2, overdiagnosis of tumor extension (see Table 2). In nine cases in group 2, histology-proven fibrocystic change, apocrine metaplasia, and ductal or lobular hyperplastic area showed a low ADC value and did not include a carcinoma component (Fig. 3). These

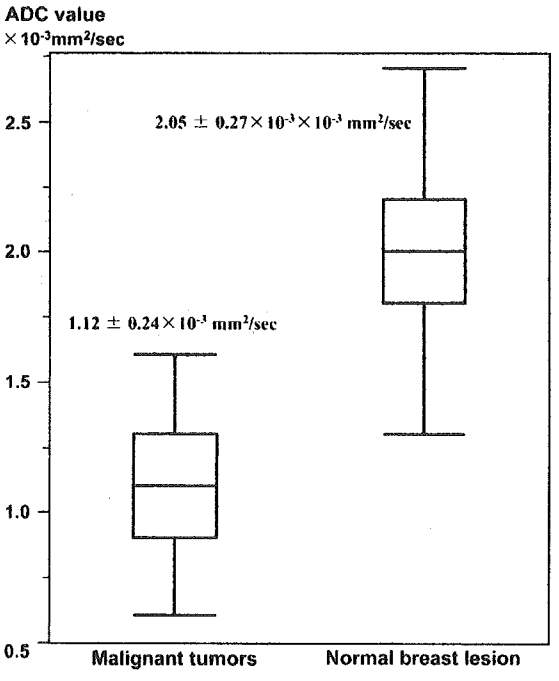

FIGURE 1. Comparison of ADC values between malignant lesions and normal lesions.

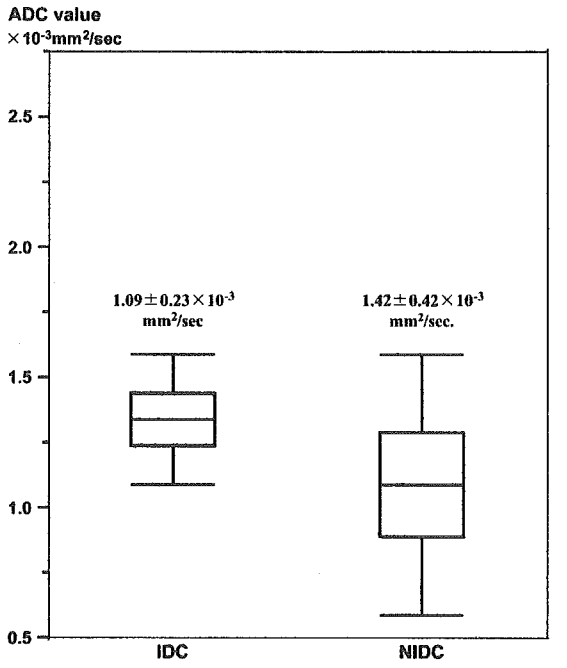

FIGURE 2. Correlation of ADC values between IDC and NIDC. IDC values were lower than NIDC values.

cases showed segmental and spotty distribution of low ADC value around the primary malignant lesion. The mean ADC value of these proliferative changes was 1.34×10^{-3} mm^2/s (range $1.1–1.5 \times 10^{-3}$ mm^2/s).

Three cases were in group 3 and one case was in group 4 (Table 3). Two cases in group 3 were invasive lobular carcinoma. The ADC map in these cases showed a low ADC area on the solid core of the tumor. However, the ADC map did not depict the sparse distribution and small foci of lobular carcinoma widely spread in the mammary gland and fat tissue (Fig. 4). One case in group 3 and the one case in group 4 showed comedo-type ductal carcinoma in situ (DCIS), which contained remarkable hemorrhage and necrosis. Also, hemosiderin deposition around ducts was observed in the pathologic figure of the group 4 case (Fig. 5).

DISCUSSION

DWI has a new potential in the approach to the biologic and structural character of tissues. Previous reports suggested that a low ADC value might indicate high cell density, dense mucus tissue, and fibrosis.[11–13,16,17–19] Although the mechanism of DWI appearance is still uncertain, the use of DWI for diagnosis and differentiation of diseases has been recently spreading from the central nerve system to other organs.[10–14,16,17,20] This advance is due largely to the EPI sequence, which shortens the scan time and minimizes motion artifact.[21] Our results in the present study showed 95% sensitivity for malignant tumors by DWI with only a 1-minute scan time, which is equivalent to the findings of Guo et al[16] and Kuroki et al.[20] DWI showed high sensitivity for breast cancer and a short scan time.

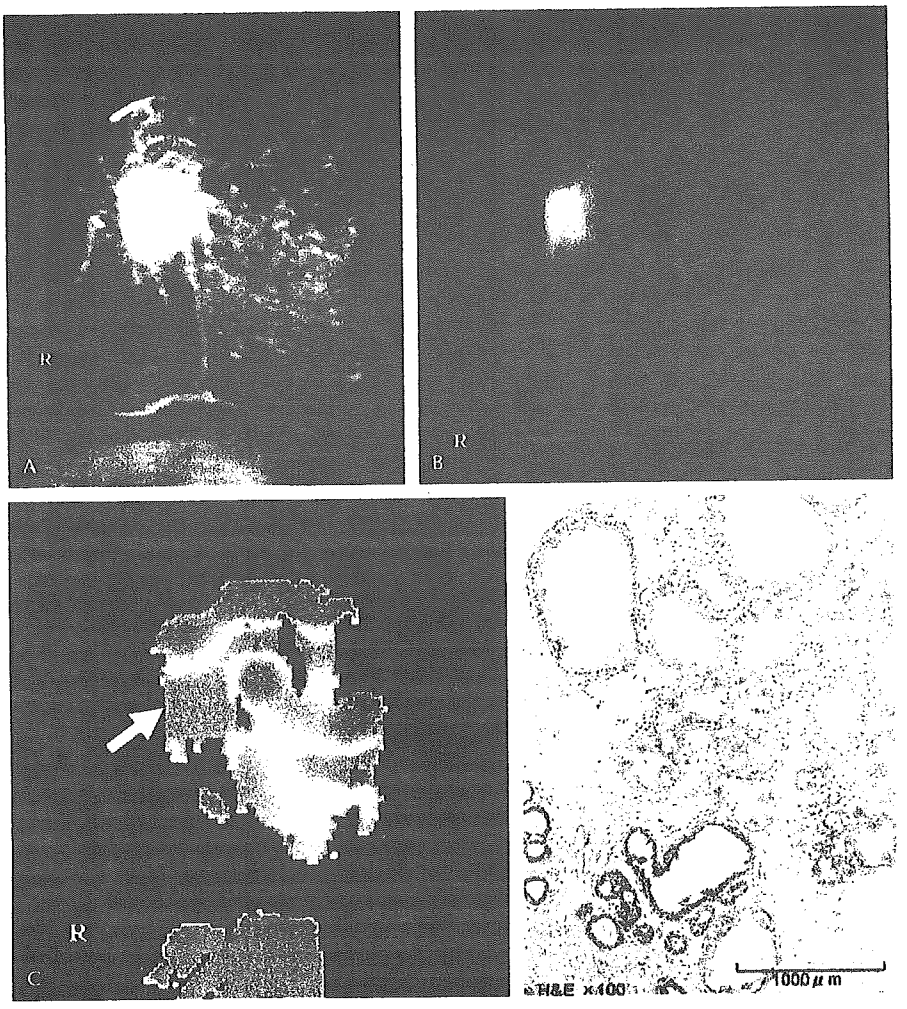

FIGURE 3. A case of solid tubular carcinoma that showed a low ADC area around the mass lesion. A, Maximum intensity projection (MIP) image of subtraction image. An enhanced mass lesion is evident in the right area. There is diffuse nodular enhancement around the mass lesion. B, DWI in the axial plane. There is a high-intensity lesion on the right side that demonstrates the carcinoma lesion (b-value = 750 s/mm^2). C, Axial plane ADC map (b-value = 750 s/mm^2). The green area (arrow) indicates the low ADC area (ADC < 1.3). The area of low ADC value in the right side represents IDC (ADC value = 1.1 × 10^{-3} s/mm^2). In the surrounding green area, ADC value = 1.5 × 10^{-3} s/mm^2. D, Histologic appearance of the benign hyperplasia adjacent to carcinoma in concordance with the area of low ADC value (H&E, ×100). Marked apocrine metaplasia is seen.

In 78% of our cases, carcinoma spread was almost precisely detected by the ADC map. This result shows that DWI could be used for the preoperative examination of cancer extension.

In this study, the b-value was 750 s/mm^2, which is lower than recommended. By using a higher b-value, the ADC value would be less affected by perfusion, and the ADC discrepancy between malignant and benign lesions could be larger, as the perfusion effect would be much more in malignant lesions than benign lesions because of tumor angiogenesis.[2] However, a high b-value would require a long TE and would cause distortion of the image. Using new technology such as parallel imaging, DWI will provide higher sensitivity and detectability for breast cancer.[8] Because our study showed a high sensitivity for malignancy and cancer spread, a b-value of 750 s/mm^2 was sufficient to retain image quality and to obtain a high sensitivity for the diagnosis of breast cancer.

EPI has a magnetic susceptibility artifact. One of our false-negative cases and one underestimated case showed hemorrhage and hemosiderin deposition in the area where the ADC map did not show low ADC value despite the existence of a carcinoma compartment. It was considered that a blood component caused a magnetic susceptibility artifact and resulted in a high ADC value. This type of false-negative result will be predictable because T1-weighted images showed high-intensity lesions where the hemorrhagic component was present in these two cases (see Fig. 5); also, it is possible that bloody

TABLE 3. Histopathologic Detail of Groups 3 and 4

Case	Group	Group Description	Tumor Size (mm)	Pathology
1	3	Underestimate	20 × 10	Lobular Ca
2	3	Underestimate	20 × 20	Comedo-type DCIS with hemorrhage and necrosis
3	3	Underestimate	25 × 15	Lobular Ca
4	4	False-negative	20 × 20	Intracystic papillary Ca surrounded by comedo-type DCIS with hemosiderin deposition and hemorrhage

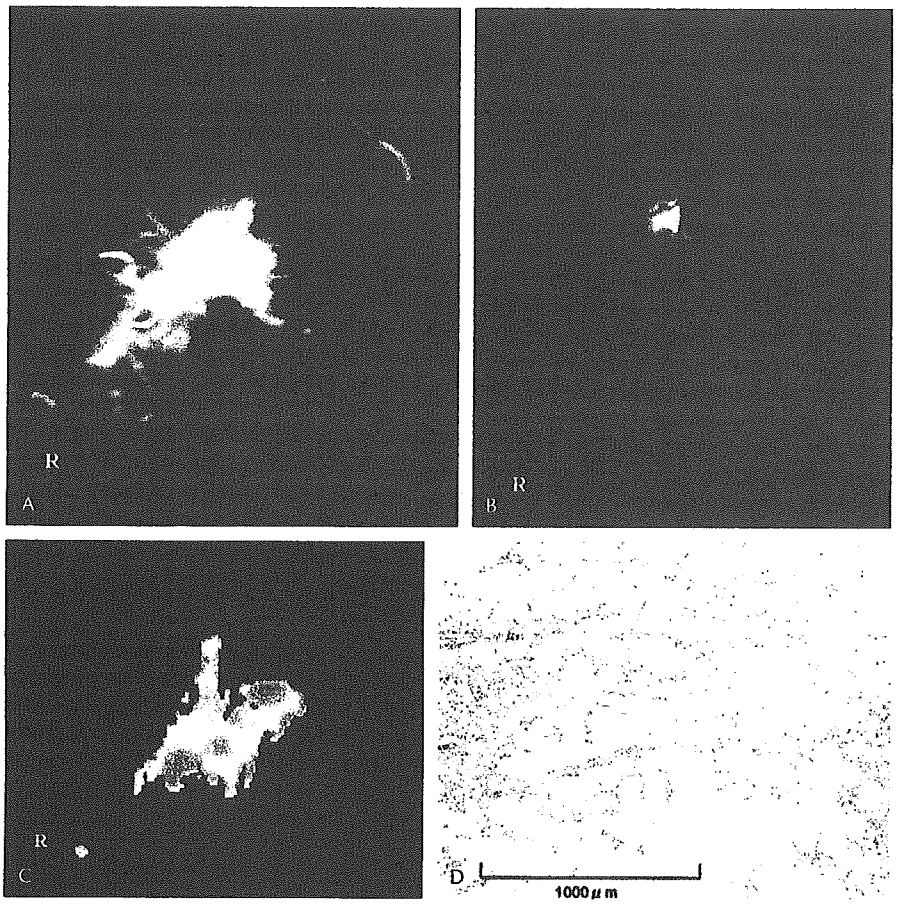

FIGURE 4. A case of lobular carcinoma with widespread carcinoma component over mammary gland and fatty tissue. A, MIP image of subtraction image. There is an enhanced tumor with segmental nodular enhancements around which is an extensively invasive component. B, DWI shows localized high-intensity lesion in Carea area (b-value = 750 s/mm^2). C, ADC map shows ADC decrease referring to the center of the tumor. Invasive compartment around the center of the tumor is not depicted on the ADC map. D, Histologic appearance of the area where the ADC map did not show ADC reduction (H&E, ×100). Sparse and scattered distribution of cancer cells is shown in the fat tissue.

secretion will be observed on physical examination in such cases. In addition, these two cases had necrotic compartment referring to comedo-type DCIS. Noguchi et al mentioned high ADC values of necrosis in brain tumors.[11] Conversely, brain abscess showed a low ADC value. They hypothesized that the reason for this discrepancy was viscosity differences: the viscosity is low in tumor necrosis but high in brain abscess because of the packing of molecules and leukocytes. In our cases, though a low ADC area in DCIS lesions would mainly be affected by susceptibility artifacts, necrosis may have had some influence on high ADC values.

Another factor that affects ADC values is the architecture of tumors. In our study, the ADC map did not detect the sparse distribution of lobular carcinoma in two cases. Guo et al reported that a 4-mm-diameter DCIS was not visualized on DWI.[16] The distribution of scattering small cores as in DCIS and the marginal lesions of lobular carcinoma will be difficult to be seen on an ADC map. Spatial resolution will be one of the factors to affect the resolution of the ADC map. Guo et al[16] and Sinha et al[22] showed that the ADC value has relevance to cell density: the mean ADC value was in inverse proportion to cell density. The disparity of the ADC value between IDC and NIDC originates from cell density as well.[20]

Our study revealed that the major factor of overestimation for cancer invasion is benign proliferative change. More than half of the overdiagnosed cases showed benign proliferative change in low ADC areas where no carcinoma existed. Distribution of low ADC values referring to benign proliferative change showed a segmental and spotty distribution, similar to the one of DCIS. Moreover, the ADC value of benign proliferative lesions overlaps with that of malignant tumor. The overlap range between breast cancer and benign proliferative lesions was 1.3 to 1.5 × 10^{-3} mm^2/ sec. Although the low ADC value of benign proliferative lesions may be due to high cellularity, leukocytes, and fibrosis because of inflammatory change, the cause is still uncertain.

Among the factors that will affect ADC values are magnetic susceptibility, cellularity, tumor size and distribution, and tissue component. In addition, spatial resolution and the signal-to-noise ratio of DWI will affect the sensitivity and specificity for breast malignant lesions. However, we expect that these issues will be improved with advances in imaging instruments and software.

This study showed that DWI has high sensitivity for breast malignant tumors and has the potential to be used to analyze cancer extension. Benign proliferative change is a major factor in false-positive results and overestimation of cancer extension on the ADC map. Magnetic susceptibility and the limit of spatial resolution cased false-negative results and underestimation of tumor extension. These issues may be

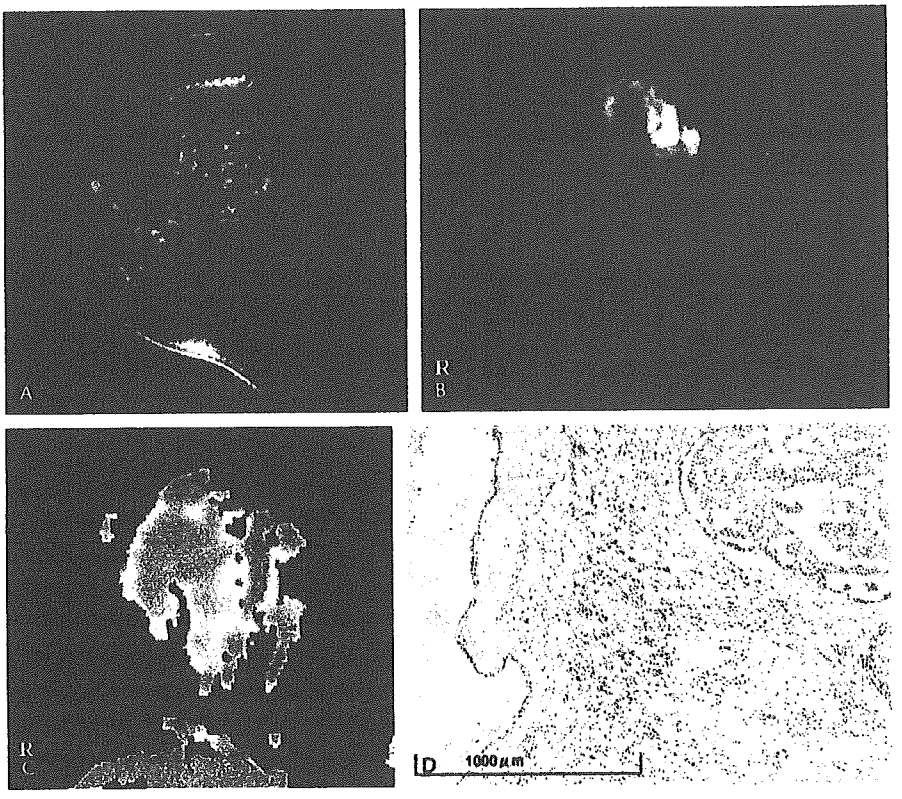

FIGURE 5. A case of intracystic papillary carcinoma with comedo-type DCIS surrounding it. A, 3D FSPGR before contrast enhancement. Note high-intensity lesion adjacent to the main tumor. It suggests a hemorrhagic lesion. B, DWI shows the main tumor as a high-intensity lesion (b-value = 750 s/mm^2). C, Axial plane ADC map shows no ADC decrease. D, Pathologic figure around the main tumor shows hemosiderin-laden macrophages adjacent to the carcinoma. There is also sporadic comedo-type DCIS distribution containing hemosiderin-laden macrophages and necrotic tissue (H&E, ×100).

solved by advances in MRI hardware and software. DWI could be one of the tools used for breast cancer diagnosis, evaluation of tumor extension, and screening because of its short scan time and high sensitivity.

REFERENCES

1. Tamaki Y, Akashi-Tanaka S, Ishida T, et al. 3D imaging of intraductal spread of breast cancer and its clinical application for navigation surgery. *Breast Cancer.* 2002;9:289–295.
2. Buadu LD, Murakami J, Murayama S, et al. Breast lesions: correlation of contrast medium enhancement patterns on MR images with histopathologic findings and tumor angiogenesis. *Radiology.* 1996;200:639–649.
3. Bone B, Aspelin P, Brouge L, et al. Sensitivity and specificity of MR mammography with histopathologic correlation in 250 breasts. *Acta Radiol.* 1996;37:208–213.
4. Schelfout K, Van Goethem M, Kersschot E, et al. Contrast-enhanced MR imaging of breast lesions and effect on treatment. *Eur J Surg Oncol.* 2004; 30:501–507.
5. Leach MO. Assessing response to treatment in breast cancer using magnetic resonance. *J Exp Clin Cancer Res.* 2002;21:39–45.
6. Rieber A, Brambs HJ, Gabelmann A, et al. Breast MRI for monitoring response of primary breast cancer to neo-adjuvant chemotherapy. *Eur Radiol.* 2002;12:1711–1719.
7. Kaiser WA, Mittelmeier O. MR mammography in patients at risk. [in German] *Rofo Fortschr Geb Rontgenstr Neuen Bildgeb Verfahr.* 1992; 156:576–581.
8. Siegmann KC, Müller-Schimpfle M, Schick F, et al. MR imaging-detected breast lesions: histopathologic correlation of lesion characteristics and signal intensity data. *AJR Am J Roentgenol.* 2002;178:1403–1409.
9. Orel SG, Schnall MD, LiVosi VA, et al. Suspicious breast lesions: MR imaging with radiologic-pathologic correlation. *Radiology.* 1994;190: 485–493.
10. Warach S, Boska M, Welch MK. Pitfalls and potential of clinical diffusion-weighted MR imaging in acute stroke. *Stroke.* 1997;28:481–482.
11. Noguchi K, Watanabe N, Nagayoshi T, et al. Role of diffusion-weighted echo planar MRI in distinguishing between brain abscess and tumour: a preliminary report. *Neuroradiology.* 1999;41:171–174.
12. Kim T, Murakami T, Takahashi S, et al. Diffusion weighted single-shot echoplanar MR imaging for liver disease. *AJR Am J Roentgenol.* 1999; 173:393–398.
13. Namimoto T, Yamashita Y, Sumi S, et al. Focal liver masses: characterization with diffusion-weighted echo planar MR imaging. *Radiology.* 1997;04:739–744.
14. Kuroki S, Nasu S, Murakami K, et al. Pancreatic cancer on DWI. *Nippon Acta Radiol.* 2003;63:S184.
15. Englander SA, Ulug AM, Brem R, et al. Diffusion imaging of human breast. *NMR Biomed.* 1997;10:348–352.
16. Guo Y, Cai YQ, Cai ZL, et al. Differentiation of clinically benign and malignant breast lesions using diffusion-weighted imaging. *J Magn Reson Imaging.* 2002;16:172–178.
17. Lyng H, Haraldseth O, Rofstad K. Measurement of cell density and necrotic fraction in human melanoma xenografts by diffusion weighted magnetic resonance imaging. *Magn Reson Med.* 2000;43:828–836.
18. Sugahara T, Korogi Y, Kochi M, et al. Usefulness of diffusion weighted MRI with echo-planner technique in the evaluation of cellularity in gliomas. *J Magn Reson Imaging.* 1999;9:53–60.
19. Noguchi K, Watanabe N, Nagayoshi T, et al. Role of diffusion weighted echo-planner MRI in distinguishing between brain abscess and tumour: a preliminary report. *Neuroradiology.* 1999;41:171–174.
20. Kuroki Y, Katsushiro N, Kuroki S, et al. Diffusion-weighted imaging of breast cancer with the sensitivity encoding technique: analysis of apparent diffusion coefficient value. *MRMS.* 2004;3:79–85.
21. Bammer R. Basic principles of diffusion-weighted imaging. *Eur J Radiol.* 2002;45:169–184.
22. Sinha S, Lucas-Quesada FA, Sinha U, et al. In vivo diffusion-weighted MRI of the breast: potential for lesion characterization. *J Magn Reson Imaging.* 2002;15:693–704.

Magnetic Resonance in Medical Sciences, Vol. 4, No. 1, p. 35–42, 2005

MAJOR PAPER

ADC Mapping of Benign and Malignant Breast Tumors

Reiko WOODHAMS[1]*, Keiji MATSUNAGA[1], Shinichi KAN[1], Hirofumi HATA[1], Masanori OZAKI[4], Keiichi IWABUCHI[2], Masaru KURANAMI[3], Masahiko WATANABE[3], and Kazushige HAYAKAWA[1]

[1]*Department of Radiology,* [2]*Department of Pathology,* [3]*Department of Surgery, Kitasato University School of Medicine*

[4]*Department of Medical Engineering and Technology, Kitasato University School of Allied Health Science*

1-15-1 Kitasato, Sagamihara, Kanagawa 228-8555, Japan

(Received March 10, 2005; Accepted May 18, 2005)

Purpose: The purpose of this study was to investigate the utility of diffusion-weighted imaging (DWI) and the apparent diffusion coefficient (ADC) value in differentiating benign and malignant breast lesions and evaluating the detection accuracy of the cancer extension.

Materials and Methods: We used DWI to obtain images of 191 benign and malignant lesions (24 benign, 167 malignant) before surgical excision. The ADC values of the benign and malignant lesions were compared, as were the values of noninvasive ductal carcinoma (NIDC) and invasive ductal carcinoma (IDC). We also evaluated the ADC map, which represents the distribution of ADC values, and compared it with the cancer extension.

Results: The mean ADC value of each type of lesion was as follows: malignant lesions, $1.22 \pm 0.31 \times 10^{-3}$ mm^2/s; benign lesions, $1.67 \pm 0.54 \times 10^{-3}$ mm^2/s; normal tissues, $2.09 \pm 0.27 \times 10^{-3}$ mm^2/s. The mean ADC value of the malignant lesions was statistically lower than that of the benign lesions and normal breast tissues. The ADC value of IDC was statistically lower than that of NIDC. The sensitivity of the ADC value for malignant lesions with a threshold of less than 1.6×10^{-3} mm^2/s was 95% and the specificity was 46%. A full 75% of all malignant cases exhibited a near precise distribution of low ADC values on ADC maps to describe malignant lesions. The main causes of false negative and underestimation of cancer spread were susceptibility artifact because of bleeding and tumor structure. Major histologic types of false-positive lesions were intraductal papilloma and fibrocystic diseases. Fibrocystic diseases also resulted in overestimation of cancer extension.

Conclusions: DWI has the potential in clinical appreciation to detect malignant breast tumors and support the evaluation of tumor extension. However, the benign proliferative change remains to be studied as it mimics the malignant phenomenon on the ADC map.

Keywords: ***breast cancer, breast MRI, DWI, fibrocystic disease, susceptibility artifact***

Introduction

The latest advancements in MRI (magnetic resonance imaging) technology have greatly expanded the utility of diffusion-weighted imaging (DWI) in the examination of various organs and diagnosis of various disorders.[1-4] DWI has already been applied in the important clinical use of diagnosis of brain ischemia and for differentiating brain abscess from metastatic brain tumor.[5,6] Moreover several studies have revealed the usefulness of DWI in characterizing brain lesions and tumors of the liver, pancreas, and ovary.[7-12] The greatest advantage of DWI in the diagnosis of neoplasm is that DWI reflects the biological character of the tissue. Furthermore, an enhancing material is not necessary. DWI is already achieving the stage of clinical application.

The use of DWI for breast cancer diagnosis is also recently being considered in clinical application.[3,13-15] Some authors showed lower ADC values for breast cancer compared with normal breast tissue. Y. Kuroki et al. also showed the utility of

*Corresponding author, Phone: +81-42-778-8453, E-mail: reiko99@db3.so-net.ne.jp

Table 1. Distribution of mean ADC values in histologic types of benign lesions

Benign Lesions	n	Mean ADC value (10^{-3} mm^2/s)
Fibrocystic disease	8	1.65 ± 0.28
Intraductal papilloma	6	1.32 ± 0.15
No evidence of malignancy	3	2.50 ± 0.44
Phyllodes benign	3	2.00 ± 0.45
Fibroadenoma	2	1.10 ± 0.23
Atypical hyperplasia	1	1.7
Granuloma (after plastic surgery)	1	0.7
Total	24	

Table 2. Distribution of mean ADC values in histologic types of breast cancer

Malignant Lesions	n	Mean ADC value (10^{-3} mm^2/s)
IDC		
Solid tubular Ca	43	1.16 ± 0.26
Papillotubular Ca	38	1.17 ± 0.29
Scirrhous Ca	34	1.17 ± 0.26
Lobular Ca	11	1.07 ± 0.26
Malignant Phyllodes	3	1.67 ± 0.59
Medullary Ca	2	1.05 ± 0.28
Invasive micropapillary Ca	2	1.15 ± 0.21
SCC	2	1.3
Mucinous Ca	2	1.75
Adenoid cystic Ca	1	1.0
NIDC or predominant NIDC		
DCIS	27	1.36 ± 0.20
Intracystic papillary Ca	2	2.6 ± 0.14
Total	167	

parallel imaging for breast DWI and displayed the significant difference between the ADC of malignant tumor and benign tumor.[15] Y. Guo et al. interpreted the correlation between cell density and ADC value and showed the inverse proportion between them.[3]

We investigate the usefulness of DWI for qualitative diagnosis of the breast and verify the sensitivity, specificity, and accuracy of DWI for breast cancer. We also evaluate the efficacy of the ADC map for assessing cancer extension.

Materials and Methods

Subjects: The subjects comprised 190 patients with a total of 191 lesions who had undergone MRI for breast examination due to tumor palpability, bloody secretion, calcification on mammography, and follow up after plastic surgery. All patients were female and aged between 14 and 88 years (mean age: 53 years). All patients underwent surgical resection and received definite pathological diagnosis.

Histological detail: Findings were 24 benign lesions, including 7 ductal hyperplasia, 1 sclerosing adenosis, 6 intraductal papilloma, 1 atypical ductal hyperplasia, 3 benign phyllodes tumor, 2 fibroadenoma, 1 granuloma, and 3 with no evidence of abnormality (Table 1). Malignant lesions totaled 167, including 43 solid-tubular carcinoma, 38 papillotubular carcinoma, 34 scirrhous carcinoma, 27 ductal carcinoma in situ (DCIS), 11 invasive lobular carcinoma, 2 malignant phyllodes tumor, and 14 others (Table 2). The mean size of the benign lesions was 34.0 mm (from 5 to 110 mm) and that of malignant lesions was 36.8 mm (from 7 to 60 mm).

MRI protocol: MRI was performed with a General Electric (GE) Signa CV/i 1.5T ver. 9.1 MRI unit equipped with a breast coil (surface coil). Prior to DWI, fast recovery fast spin echo (FRFSE) with CHESS was performed for fat saturation in the sagittal plane. After DWI was performed in the axial plane, 3 dimensional fast spoiled gradient recalled acquisition in the steady state (3DFSPGR) with Spec IR for fat saturation in the sagittal plane was performed before and after administration of gadopentetate dineglumine (0.2 mmol/kg). Subtraction images were produced with 3DFSPGR for identification of enhancement. 2DFSPGR with CHESS in the axial plane was performed after enhancement. Imaging parameters were as follows: 2DFRFSE (TR 3000, eff TE 85, 256 × 192, 3NEX), DWI [spin echo-single shot echo planar image (EPI) and motion probing gradient (MPG) were applied along the X, Y and Z axes (isotopic DWI) before and after the 180° pulses to obtain the images used for synthesizing isotropic images; b-values were 0 and 750 s/mm^2, TR/TE: 5000/61.8, image matrix: 128 × 128, field of view: 320 × 240 mm, slice thickness: 6 mm, spacing: 1 mm, 5NEX, acquisition time: 100 s], 3DFSPGR (TR 5.7, TE 1.2, flip angle: 20°, image matrix: 256 × 160, 2NEX), 2DFSPGR (TR 200, TE minimum, flip angle: 90°, image matrix: 512 × 192, 3NEX).

ADC value: All ADC values were calculated according to the formula: $ADC = -(1/b)\ln(S/So)$, where So and S are the signal intensities in the region of interest (ROI), obtained with different gradient factors (b values of 0, 750, and 1000

Table 3. Categorization of the four groups of correlation between low ADC value distribution on the ADC map and tumor distribution in the pathologic figures

Group	Distribution of Low ADC Values on ADC Map	n	%
G-1	Accurate distribution	129	77
G-2	Overestimation	15	9
G-3	Underestimation	11	7
G-4	False negative	12	7
Total		167	

G-1: Low ADC area similar to tumor distribution
G-2: Low ADC area greater than tumor distribution
G-3: Low ADC area smaller than tumor distribution
G-4: No decline in ADC

s/mm^2). ADC distribution was demonstrated on an ADC color map created with Advantage Workstation ver. 4.0 (GE). The ROI was placed in the target lesion and normal breast area on the ADC map with reference to subtraction images originating from 3DFSPGR and 2DFSPGR imaging after enhancement. The ROIs of the tumor lesions were smaller than the mass size excluding the normal tissue area. The size of the ROI in the area of normal breast tissue was 10 mm in diameter. Each ROI was positioned twice with a change of location and ADC values were averaged.

ADC values of benign lesions, malignant lesions, and normal breast tissues were compared, as were those of non-invasive ductal carcinoma (NIDC) and invasive ductal carcinoma (IDC). NIDC was considered to include predominant NIDC.

On the subject of malignant cases, we determined a low ADC value for malignant lesions as being less than 1.6×10^{-3} mm^2/s. We recognized the low ADC value area by a certain color on the ADC map and compared ADC maps with pathological figures to determine the accuracy of the ADC map for cancer extension. We categorized the pattern of correlation between the distribution of ADC values on the ADC map and the cancer extension in the pathological figure into 4 groups: Group 1 (G-1), where the area of low ADC values was almost the same as the tumor extension; Group 2 (G-2), where the area of low ADC values was wider and more than twice the area of tumor extension; Group 3 (G-3), where the area of low ADC values was smaller and less than one-half the area of tumor extension; and Group 4 (G-4), where no ADC reduction was observed (Table 3).

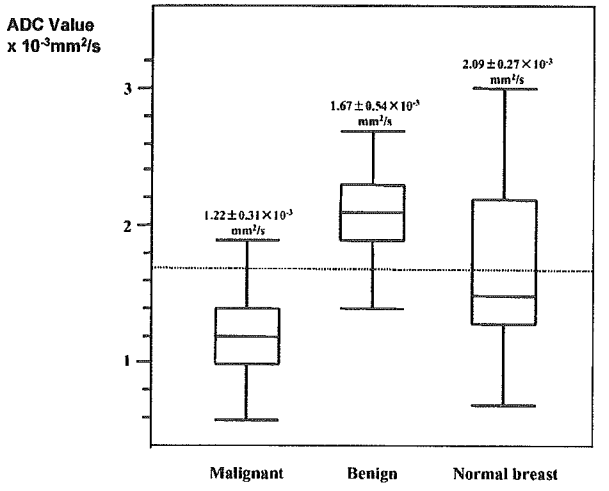

Fig. 1. Comparison among ADC values for malignant lesions, benign lesions, and normal breast tissues

Statistics

Tukey-Kramer's honesty significant difference (HSD) test was used to compare the mean ADC values of malignant tumor, benign tumor, and normal breast tissue.

The Wilcoxon signed rank sum test was used to analyze differences in the mean ADC value for significance between IDC and NIDC or predominant NIDC.

Result

Comparison of ADC values: The mean ADC value of the 167 malignant lesions was $1.22\pm0.31\times10^{-3}$ mm^2/s (ranging from 0.6 to 2.7×10^{-3} mm^2/s). The mean ADC value of the 24 benign lesions was $1.67\pm0.54\times10^{-3}$ mm^2/s (ranging from 0.7 to 3.0×10^{-3} mm^2/s), and the mean ADC value of normal breast tissue in all cases was $2.09\pm0.27\times10^{-3}$ mm^2/s (ranging from 1.4 to 3.0×10^{-3} mm^2/s). A statistically significant difference in ADC values was observed between benign tumors, malignant tumors, and normal breast tissues (Fig. 1).

The mean ADC value of IDC was $1.20\pm0.32\times10^{-3}$ mm^2/s and that of NIDC was $1.35\pm0.25\times10^{-3}$ mm^2/s. There was also significant difference ($p=0.02$) between them (Fig. 2).

Sensitivity and specificity of ADC value: With an ADC value of less than 1.6×10^{-3} mm^2/s defined as being an indicator of malignancy, 155 of the 167 malignant cases were identified as malignant lesion on the ADC map without concern for the range of ADC reduction. Sensitivity to malignant lesions was 93%. On the other hand, 13 benign cases were

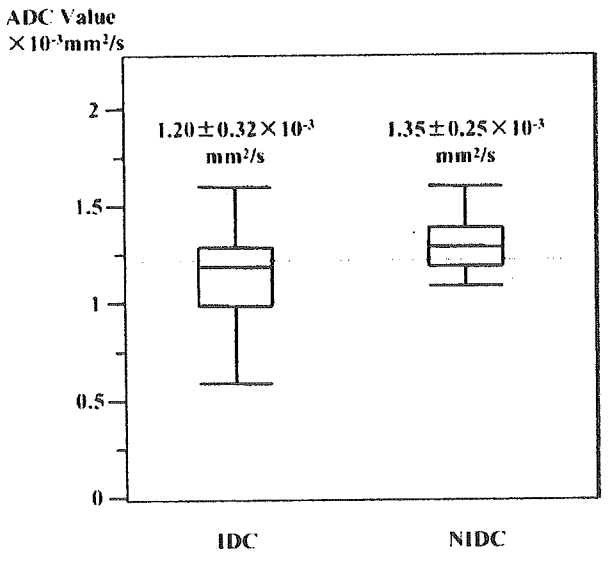

Fig. 2. Comparison between ADC values of NIDC and IDC

misdiagnosed as malignant lesions. Thus, the specificity was 46% (11/24) and the accuracy was 87% (166/191).

In 13 cases, benign lesions were misdiagnosed. The histologic details of these benign lesions were as follows: five cases of intraductal papilloma with a mean ADC value of 1.24×10^{-3} mm^2/s (ranging from 0.9 to 1.4×10^{-3} mm^2/s); three cases of fibroadenomatosis, one of ductal hyperplasia, and one of sclerosing adenosis with a mean ADC value of these lesions, fibrocystic change of 1.34×10^{-3} mm^2/s (ranging from 1.2 to 1.5×10^{-3} mm^2/s); two cases of fibroadenoma with a mean ADC value of 1.1×10^{-3} mm^2/s; and one case of granuloma with an ADC value of 0.7×10^{-3} mm^2/s.

Comparison of ADC map and histopathologic features: All malignant cases were classified into 4 groups according to the concurrence of tumor extension and distribution of low ADC values on the ADC map. A total of 129 cases were classified as G-1; 15 cases as G-2; 11 cases as G-3; and 12 cases as G-4 (Table 3).

Of the cases categorized as G-1, 11 cases represented a small compartment of DCIS foci neighboring the main tumors, which DWI did not depict. While these lesions were in the same segment as the main tumors and the sizes were less than one half as large as the main tumors, we decided to categorize such cases as G-1 (Fig. 3).

Regarding G-2, the histopathologic details of the overdiagnosed area, which showed a low ADC value of less than 1.6×10^{-3} mm^2/s instead of an absence of malignant compartment, were as follows: 1 case of apocrine metaplasia; 7 of ductal or lobular hyperplasia; 2 of blunt duct adenosis; 2 of sclerosing adenosis; 1 of fibroadenomatosis; and 2 no evidence of malignancy (Fig. 4).

With regard to G-3, the histopathologic details of the malignant component, where the ADC map did not show a low ADC value, were as follows: 4 cases showed comedo-type DCIS containing notable bleeding and necrosis, 1 case was an intracystic papillary carcinoma, 1 case showed sporadic DCIS and lobular carcinoma invasion, 2 cases were necrosis and hemorrhage section of phyllodes malignant, 2 cases were marginal zone of lobular carcinoma, and 1 case was papillotubular carcinoma. In other words, 7 cases had bleeding component in G-3. In addition, 2 cases of lobular carcinoma and 1 case of lobular carcinoma with DCIS showed sparse and small foci of tumor components in the area which the ADC map did not depict as a low ADC area (Fig. 5).

The histologic details of G-4 were as follows: 3 cases of DCIS, 2 of scirrhous carcinoma, 2 of solid tubular carcinoma, 2 of papillotubular carcinoma, and 1 each of intracystic papillary carcinoma, malignant phyllodes tumor, and mucinous carcinoma. In these cases, some notable histologic characters were seen in the specimens. Nine cases showed remarkable blood components in the specimens of malignant components (Fig. 6). In G-3 and G-4, 14 cases out of 16 with bloody components showed as high-intensity lesions in T_1-weighted images.

Discussion

According to the past reports, MRI has been confirmed as an essential tool for examination of the breasts because of its remarkably higher sensitivity with the use of enhancement material for breast carcinoma than that of ultrasound and mammography. MRI demonstrates its virtues in the research of occult cancers, where mammography and ultrasound can neither detect nor assess the cancer extension. Preoperative contrast-enhanced MRI of the breast has the potential to reveal mammographically and sonographically hidden multifocal breast carcinoma.[16-26] However, the disadvantages of MRI compared with mammography and ultrasound are the long scan times, usually 20 to 30 min, and the need for a contrast medium. In addition, the contrast material increases the cost. Furthermore, we feel that the conventional diagnostic techniques of breast MRI, morphological diagnosis and analysis of dynamic enhancement patterns, are limited to a certain degree.[27-29] On the other hand, DWI reflects some elements that affect proton diffusion, for example